Superconducting-normal phase boundary of quasicrystalline arrays in a magnetic field

Franco Nori,*† Qian Niu, Eduardo Fradkin, and Shau-Jin Chang
Physics Department, University of Illinois at Urbana-Champaign, Urbana, Illinois 61801
(Received 14 November 1986; revised manuscript received 16 September 1987)

We study the effect of frustration, induced by a magnetic field, on the superconducting diamagnetic properties of two-dimensional quasicrystalline arrays. In particular, we calculate the superconducting-normal phase boundary, $T_c(H)$, for several geometries with quasicrystalline order. The agreement between our theoretically obtained phase boundaries and the experimentally obtained ones is very good. We also propose a new way of analyzing the overall and the fine structure of $T_c(H)$ in terms of short- and long-range correlations among tiles.

A large number of experiments have studied flux quantization in two-dimensional (2D) *periodic* superconducting arrays.[1] However, several groups[2-4] have recently performed experiments with superconducting *ordered nonperiodic* structures with either fractal or quasicrystalline (QC)[5] geometry. The groups[3,4] who have studied the effect of an externally applied magnetic field on quasicrystalline arrays have constructed two types of superconducting networks: aluminum wire micronetworks[3] and an array of Josephson junctions.[4] Nevertheless, in contrast to all this considerable experimental effort,[3,4] very little theoretical work has been done on these systems.

It is the purpose of this paper to study the frustration induced in 2D quasicrystalline networks by an applied magnetic field, and its effect on their superconducting diamagnetic properties. In particular, we calculate the superconducting-normal phase boundary $T_c(H)$ for all the 2D geometries which have been studied experimentally.[3,4] The agreement between our curves and the experimental data[3,4] obtained so far is very good. Furthermore, we propose a new analytical and systematic way of analyzing the structure of the phase boundaries in terms of correlations among tiles. Conclusions obtained using this novel approach are consistent with recent measurements by Springer and Van Harlingen[4] on Josephson-junction arrays.

In these systems, a continuous variation of the applied magnetic field allows the unique possibility for a fine tuning of the geometry-induced frustration. The ratio of the elementary plaquette areas is equal to an irrational number for all four lattices considered here. This geometric constraint implies that the magnetic flux cannot satisfy quantization in all the plaquettes simultaneously. We have considered the linearized Ginzburg-Landau equations[6] (for the superconducting networks) and the linearized mean-field approximation to the frustrated XY Hamiltonian[7] (for the Josephson junction array). Both of them can be formally written[6,7] as a tight-binding Schrödinger equation $\sum_\beta J_{\alpha\beta} e^{iA_{\alpha\beta}} \psi_\beta = \epsilon \psi_\alpha$ where $A_{\alpha\beta} = 2\pi/\Phi_0 \int_\alpha^\beta \mathbf{A}\cdot d\mathbf{l}$, and $\Phi_0 = ch/2e$. The highest eigenvalue is proportional to $T_c(H)$.

The geometries considered here are (1) periodic (with 500 spacings or more) along one direction and quasicrystalline (with 60 spacings or less) in the other direction (strip geometry), (2) Penrose lattice [see Fig. 1(a)], and (3) eightfold Penrose lattice [see Fig. 1(b)]. We have considered (1) both in the Fibonacci case, which is associated with the "golden mean," and the "silver mean" case. The Fibonacci lattice is the 1D analog of the Penrose lattice.[5] For these two networks, the ratio of basic frequencies in the diffraction pattern is equal to the golden mean, $\tau \equiv (\sqrt{5}+1)/2 = 2\cos(\pi/5)$, and the two types of elementary plaquettes have a ratio of areas (large to small) and a population ratio (number of large to number of small tiles) both equal to τ. We have also studied the 1D analog of the 2D eightfold symmetric quasicrystalline lattice.[5] The silver mean, $\zeta = \sqrt{2}+1 = \cot(\pi/8)$, characterizes the quasiperiodicity of these two networks. The ratio of areas and the population ratio, for these two lattices, are equal to $\sqrt{2}$ and $1/\sqrt{2}$, respectively. De Bruijn[5] first gave a global prescription to generate 2D Penrose patterns. We constructed our fivefold (eightfold) Penrose lattices by projecting a five- (eight-) dimensional hypercubic grid into a 2D subspace. The centers of the hypercubes which intersect a particular hypersurface are projected into it.

In order to obtain $T_c(H)$ for the 2D Fibonacci lattice, it is convenient to use the Landau gauge $\mathbf{A} = Bx\hat{\mathbf{y}}$, in which

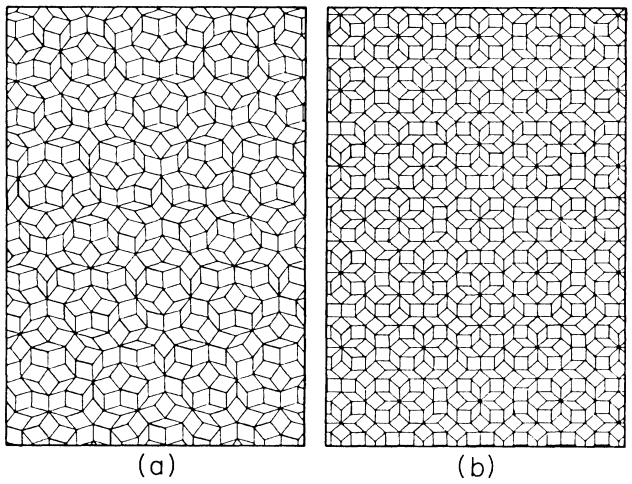

FIG. 1. (a) Portion of a Penrose pattern; (b) portion of an eightfold Penrose pattern.

an eigenfunction of our tight-binding equation takes the product form $\eta_{nm}=\psi_n e^{ikm}$, where ψ_n satisfies the 1D equation

$$\frac{2k_BT}{J}\psi_n=\psi_{n+1}+\psi_{n-1}+2\cos(2\pi f x_n-k)\psi_n \ ,$$

with $f=\Phi_s/\Phi_0$ (or $f\tau$) being the reduced magnetic flux, i.e., the magnetic flux through a small (large) cell divided by the flux quantum. For a fixed value of k, we numerically solve the above equation for the largest eigenvalue, which is then maximized by varying k in the range $(0,\pi)$ to find the transition temperature.

The transition from a *periodic* phase boundary $T_c(H)$ to the richly structured one associated with an underlying QC geometry can be followed in Fig. 2. The associated lattices have a strip-type geometry. The ratio of the elementary plaquette areas is equal to the golden mean. The minima and maxima of the $T_c(H)$ curve, for the periodic ladder geometry with only one type of cell [Fig. 2(a)] are quadratic. However, the local maxima and minima for the quasicrystalline strip systems [Figs. 2(b)–2(e)] tend, in general, to be more peaked (cusplike). This suggests that one-cell effects are responsible for the quadratic (parabolic) extrema, meanwhile the cusplike behavior is due to the collective effect of many cells. Figure 2(b) shows the $T_c(H)$ curve for a strip with two types of elementary plaquettes. From it, we note that only the main features of the 2D Fibonacci and Penrose lattices phase boundaries are essentially determined by the irrationality of the ratio

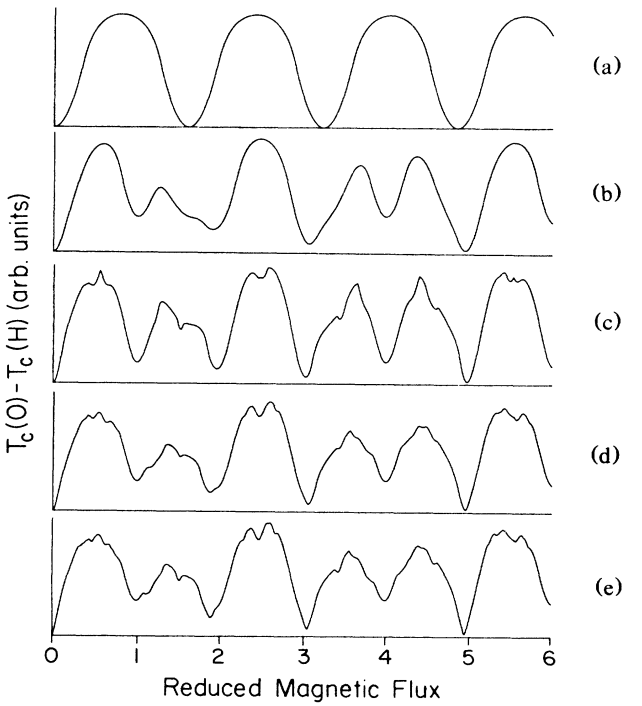

FIG. 2. Phase boundary for lattices with strip-type geometry. The number of quasicrystalline spaced vertical lines is equal to successive Fibonacci numbers: (a) 2 vertical lines (ladder network), (b) 3, (c) 5, (d) 8, and (e) 13.

of the elementary plaquette areas. If we increase the number of tiles, we obtain more and more fine structure. Below, we will come back to this point through analytical means.

As noted above, the use of a periodic direction *greatly* simplifies the calculations. However, neither the Penrose nor the eightfold Penrose lattices have periodic directions. Obtaining $T_c(H)$ for these lattices is far more difficult since these two systems *cannot* be simplified by using translational invariance and, therefore, the problem needs to be tackled directly. We have numerically solved the linearized Ginzburg-Landau equations for a Penrose lattice with 301 nodes (dotted line in Fig. 3) and for an eightfold Penrose lattice with 329 nodes (dotted line in Fig. 4). This is equivalent to solving the linearized mean-field equations for the XY Hamiltonian, or solving the electronic tight-binding problem, and then plotting the edge state versus magnetic field. Our choice of gauge was

$$A_{\alpha\beta}=\frac{2\pi}{\Phi_0}B(y_\beta-y_\alpha)(x_\alpha+x_\beta)/2 \ ,$$

where x_α and y_α are the coordinates of the αth node. The continuous line in Fig. 3 is experimental data obtained by Springer and Van Harlingen[4] for an array of 14000 weakly coupled superconducting islands fabricated using direct-write electron-beam lithography. They measured the voltage across the sample [which follows the behavior of $-T_c(H)$] versus applied transverse magnetic field. In Fig. 4 we have plotted our theoretical curve and their data, obtained for a voltage bias of around 40 nV. The agreement between them is very good. For the 2D Fibonacci geometry, and also for the Penrose array case, an average flux of one flux quantum per elementary tile corresponds[3] to an applied magnetic field of $H_0=\Phi_0(1+\tau^{-2})^{-1}/a_s$ where a_s = area of a small tile. An arrow in Fig. 3 indicates the small dip associated with this field ($H/H_0=1$). Also, the average applied field in order to have $N_l(N_s)$ flux quanta in every large (small) tile is $H=\Phi_0(N_s+\tau N_l)(1+\tau^2)^{-1}/a_s$. Therefore, the arrangements of the flux quanta[3] on the array are $(N_s,N_l)=(1,1)$, (1,2), (2,3), and (3,5) for the indicated values of the magnetic field, i.e., $H/H_0=1$, τ, τ^2, and τ^3, respectively.

The continuous line in Fig. 4 is experimental data obtained by Behrooz *et al.*[3] The arrow indicates the magnetic field corresponding to one-flux quantum in each elementary tile $H_0=\Phi_0(1+\sqrt{2})/(2a_s)$. The fields $H=\Phi_0(N_l+\sqrt{2}N_s)/2a_s$ have been indicated by $(N_l,N_s)=(1,1)$, (3,2), and (7,5) for $H/H_0=1$, ζ, and ζ^2, respectively. The fields corresponding to $n+m\zeta$ for $|n|,|m|<4$ (see Fig. 4) account for most of the theoretical and experimental fine structure.

So far, all our theoretical data were obtained numerically. However, we have also employed a novel way to obtain and explain the basic features of $T_c(H)$. This approach, based on the Lanczos method,[8] is designed to approximate the largest eigenvalue [to be denoted as $E_0(H)$] for our eigenvalue equations. As we will see, this method is not only simple but also makes explicit the physical origin of the peaks and valleys of various sizes in $T_c(H)$. First, we choose a state ψ_1 which is uniform on the lattice. Afterwards, a second state ψ_2 is obtained as

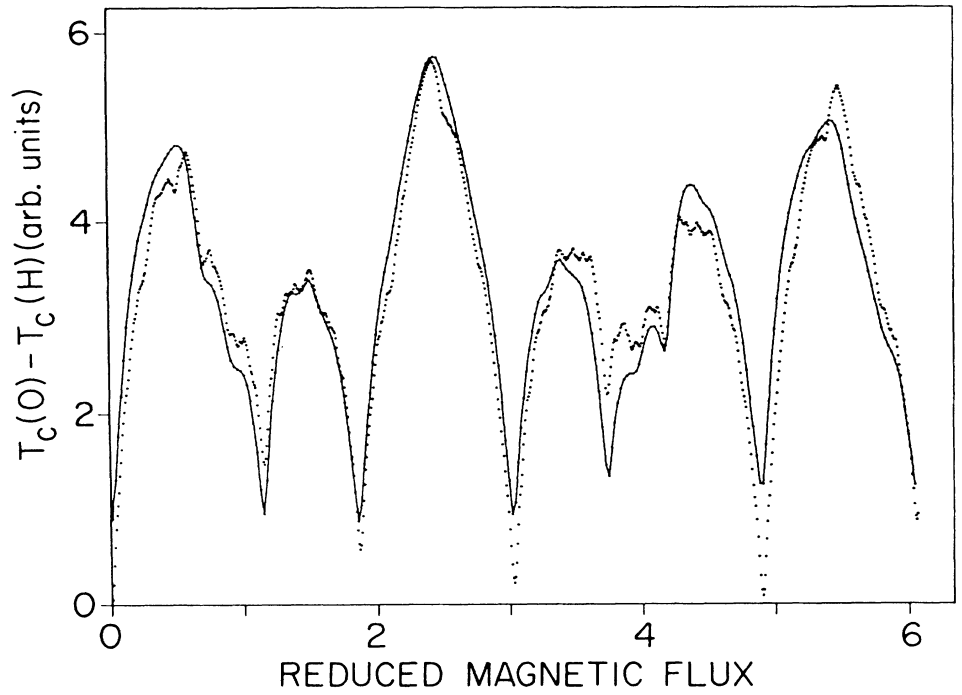

FIG. 3. Superconducting-normal phase boundary for the Penrose pattern. The solid line is experimental data for a Josephson-junction array (Ref. 4), and the points are our theoretically obtained values for a lattice with 301 nodes. The vertical axis represents voltage (10 nV) for the experimental data, and $T_c(0)-T_c(H)$ (arbitrary units) for the theory.

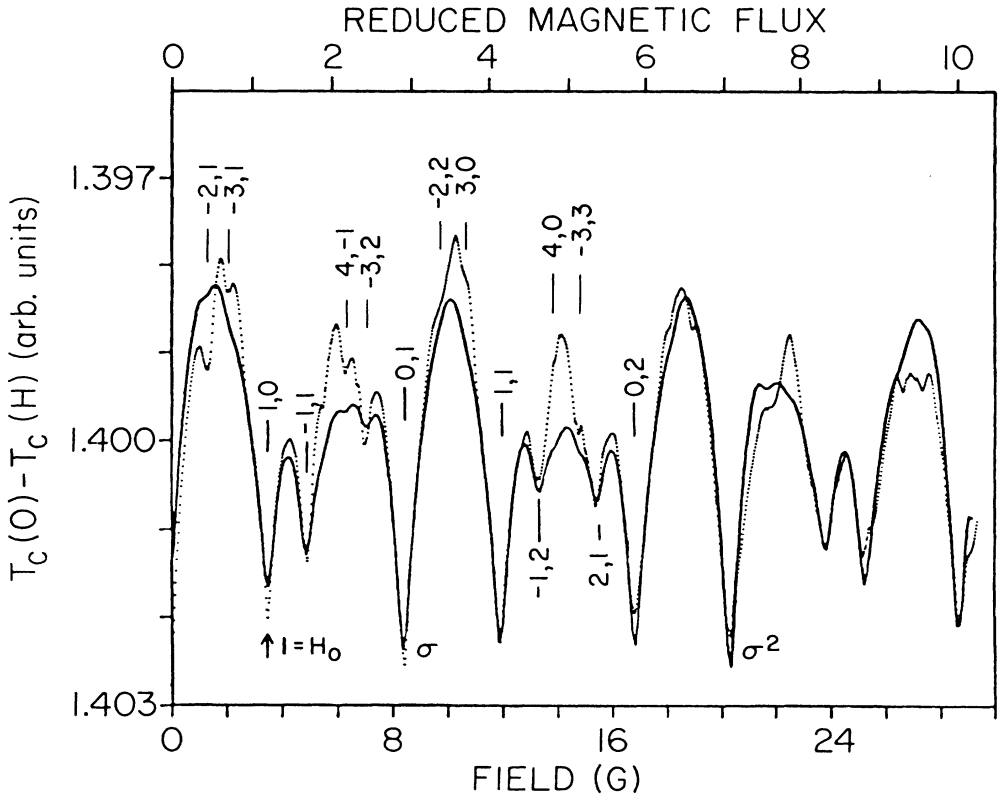

FIG. 4. Phase boundary, $T_c(0)-T_c(H)$, for the eightfold Penrose pattern. The solid line is experimental data (K) for an aluminum wire micronetwork (Ref. 3), and the points are our theoretically obtained values (arbitrary units) for a lattice with 329 nodes.

$Q_1(\hat{H}\psi_1)$, where Q_1 projects off the space spanned by ψ_1. If we replace the full Hamiltonian $\hat{H}$ by its restriction $\hat{H}_2$ on the linear manifold spanned by $\{\psi_1,\psi_2\}$, then the larger eigenvalue of $\hat{H}_2$ [which approximates $E_0(H)$] gives a fairly good result in locating the relative heights of the main peaks and dips of the $T_c(H)$ curve. If we go one step further, i.e., to define $\psi_3=Q_2Q_1(\hat{H}\psi_2)$ and replace $\hat{H}$ by its restriction $\hat{H}_3$ on the linear manifold spanned by $\{\psi_1,\psi_2,\psi_3\}$, then the largest eigenvalue of $\hat{H}_3$ gives a much better approximation to $E_0(H)$ and most of the fine structure is reproduced, in addition to the main peaks and dips.

In general, higher-order truncations of the Hamiltonian produce better results, revealing finer structures. In order to make the following discussion more specific, we will now consider a strip-type geometry as an example. A uniform state ψ_1 generates the following equations:

$$\hat{H}\psi_1=2\psi_1+2\psi_2,\quad \hat{H}\psi_2=\psi_1+C\psi_2+\psi_3\ ,$$

$$\hat{H}\psi_3=D\psi_2+F\psi_3+\psi_4,\ \ldots\ ;$$

where

$$C=2\langle\cos(2\pi fL_n)\rangle,\quad D=3-C^2+2\langle\cos[2\pi f(L_n+L_{n+1})]\rangle\ ,$$

$$F=\{C^3-C+2\langle\cos[4\pi f(L_n+L_{n+1})]\rangle-4C\langle\cos[2\pi f(L_n+L_{n+1})]\rangle+2\langle\cos[2\pi f(L_n+L_{n+1}+L_{n+2})]\rangle\}/D\ .$$

We have used the Landau gauge as before, and the angular brackets denote averages along the horizontal direction (L_n are the lattice spacings). For instance, for the particular case of the Fibonacci network:

$$\langle\cos[2\pi f(L_n+L_{n+1})]\rangle=\frac{2}{\tau^2}\cos[2\pi f(L+S)]+\frac{1}{\tau^3}\cos(4\pi fL)$$

and

$$\langle\cos[2\pi f(L_n+L_{n+1}+L_{n+2})]\rangle=\left[\frac{1}{\tau}+\frac{1}{\tau^3}\right]\cos[2\pi f(2L+S)]+\frac{1}{\tau^4}\cos[4\pi f(L+2S)]\ .$$

The largest eigenvalues, which approximate $T_c(H)$, for the second-, third-, and fourth-order truncation of the Hamiltonian have been plotted in Fig. 5. The second-order truncation is already very good at reproducing the overall structure. As we proceed to higher orders, finer structure begins to emerge and develop. In order to see why this is the case, note that in the second-order truncation only the single-cell statistics (through C) comes in, while in the third-order truncation, correlations between *nearest* and *next*-nearest neighboring cells are involved (through D and F), and the fourth-order truncation depends on even *longer*-range correlations. We have therefore *proved*, that the overall structure in $T_c(H)$ is a result of single-cell statistics. The above relations also prove, by considering successive higher-order truncations, that longer-range correlations among cells are responsible for the finer structure. This result is consistent with experimental[4] results obtained from the evolution of fine structure in Penrose lattices as a function of voltage bias. A complete and detailed exposition of this approach will be presented in full length elsewhere[9] including also the computed $T_c(H)$ curves for all the geometries studied experimentally.[3]

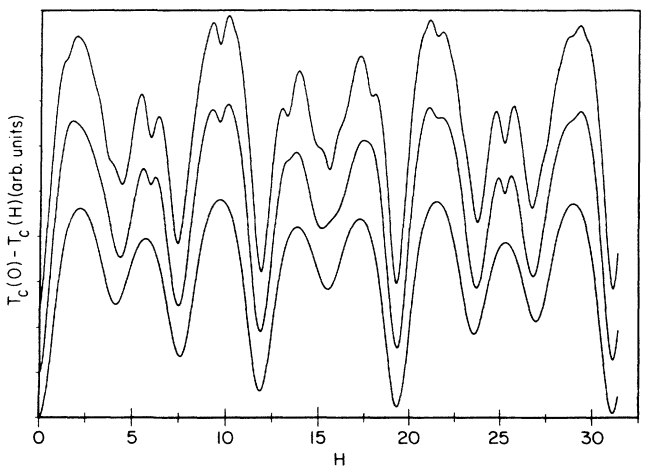

FIG. 5. Largest eigenvalues, obtained by using the Lanczos method, of the operators $\hat{H}_2$ (bottom), $\hat{H}_3$, and $\hat{H}_4$ (top) vs H for the 2D Fibonacci lattice. The vertical axis represents $T_c(0)-T_c(H)$ in arbitrary units. The curves have been shifted vertically in order to visualize them better.

The principal results we have obtained are (1) numerical calculations, which did not require a single adjustable parameter, of the superconducting-normal phase boundary for the quasicrystalline systems fabricated by several experimental groups, (2) a very good agreement between our theoretical results and the experimental ones, and (3) a proposed new analytic and *systematic* way of analyzing $T_c(H)$ which for the first time explicitly shows, in a detailed and specific manner, the way short-range correlations among tiles affect the main peaks, and the way longer-range correlations generate finer structure. Finally, some concluding comments are necessary. In our analysis, we have neglected superconducting fluctuations. Nevertheless, we do not expect them to be very important here because it is known that periodic superconducting arrays[1] in a transverse magnetic field display mean-field-like behavior. On the other hand, the size of the lattices we have studied is either one or two orders of magnitude smaller than the ones studied experimentally. We believe that this factor, together with the imperfections of the fabricated structures (e.g., the nonuniform width of the wires), accounts for most of the discrepancies between theory and experiment. Also, the finite width of the strands and the finite measurement current through the sample may smooth out some of the unobserved fine structure.

We are very grateful to D. Van Harlingen, K. Springer, and P. M. Chaikin for useful discussions and for sharing with us their published and unpublished data. F.N. acknowledges the National Center for Superconducting Applications for partial support and M. Burns, A. Lopez, and D. Stroud for conversations. Q.N. thanks M. Stone for useful discussions. This research has used the computing facilities at the Materials Research Laboratory, University of Illinois, and was supported by the National Science Foundation through Grants No. MRL-83-16981, No. DMR-84-15063, and No. PHY87-01775.

---

*Also at the Materials Research Laboratory and National Center for Supercomputing Applications, University of Illinois, Urbana, IL 61801.

†Present address: Institute for Theoretical Physics, University of California, Santa Barbara, CA 93106.

[1]B. Pannetier *et al.*, Phys. Rev. Lett. **53**, 1845 (1984); R. Webb *et al., ibid.* **51**, 690 (1983); D. Resnick *et al., ibid.* **47**, 1542 (1981); Ch. Leeman *et al., ibid.* **56**, 1291 (1986); J. Kosterlitz and E. Granato, Phys. Rev. B **34**, 1026 (1986); **33**, 6533 (1986).

[2]J. M. Gordon, A. M. Goldman, J. Maps, D. Costello, R. Tiberio, and B. Whitehead, Phys. Rev. Lett. **56**, 2280 (1986).

[3]A. Behrooz, M. Burns, H. Deckman, D. Levine, B. Whitehead, and P. M. Chaikin, Phys. Rev. Lett. **57**, 368 (1986); Phys. Rev. B **35**, 8396 (1987); B. Pannetier *et al.* (unpublished).

[4]K. Springer and D. Van Harlingen, Phys. Rev. B **36**, 7273 (1987).

[5]N. de Bruijn, Ned. Akad. Wetensch. Proc. Ser. A **43**, 27 (1981); **43**, 53 (1981); D. Levine and P. J. Steinhardt, Phys. Rev. B **34**, 596, 617 (1986); for further studies of the one-dimensional analog case see, for instance, F. Nori and J. P. Rodriguez, Phys. Rev. B **34**, 2207 (1986); Q. Niu and F. Nori, Phys. Rev. Lett. **57**, 2057 (1986).

[6]S. Alexander, Phys. Rev. B **27**, 1541 (1983); R. Rammal *et al., ibid.* **27**, 2820 (1983); J. Simonin *et al.*, Phys. Rev. Lett. **56**, 2649 (1986).

[7]W. Y. Shih and D. Stroud, Phys. Rev. B **28**, 6575 (1983); **32**, 158 (1985); **30**, 6774 (1984); J. Chung, M. Y. Choi, and D. Stroud (unpublished).

[8]C. Paige, J. Inst. Math. Its Appl. **10**, 373 (1978).

[9]F. Nori and Q. Niu (unpublished).